

Charge Transport in Self-Organized π -Stacks of *p*-Phenylene Vinylene OligomersPaulette Prins,[†] Kittusamy Senthilkumar,[†] Ferdinand C. Grozema,^{*,†} Pascal Jonkheijm,[‡] Albert P. H. J. Schenning,[‡] E. W. Meijer,[‡] and Laurens D. A. Siebbeles[†]*Opto-Electronic Materials Section, DelftChemTech, Delft University of Technology, Mekelweg 15, 2629JB, Delft, The Netherlands, and Laboratory of Macromolecular and Organic Chemistry, Eindhoven University of Technology, P.O. Box 513, 5600 MB, The Netherlands**Received: June 7, 2005; In Final Form: July 15, 2005*

We have studied the mobility of charge carriers along self-organizing π -stacks of hydrogen-bonded phenylene vinylene oligomers in solution, by time-resolved microwave conductivity measurements. The value deduced for the mobility along the stacks is 3×10^{-3} and 9×10^{-3} cm²/(V s) for holes and electrons, respectively. Additionally, we have calculated the mobility along the π -stacks using a hopping model based on parameters from density functional theory. The mobility values obtained from these calculations are in good agreement with the experimental values if it is assumed that there are relatively large twist angles between neighboring molecules in the stack. It is shown that a significantly higher mobility can be attained if the twist angle between neighboring oligomers is reduced.

1. Introduction

Organic semiconductors are promising materials for use in optoelectronic devices such as field effect transistors (FET),¹ light-emitting diodes (LED),² and photovoltaic cells.³ Most organic semiconductors are based on π -conjugated molecules, ranging in size from small oligomers to polymers. The properties of individual molecules can be tailored by variations in the molecular structure, e.g., by changing the degree of conjugation in the polymer⁴ or by introduction of electronically active substituents.⁵ The effects of intermolecular interactions on the optoelectronic properties are less well established; however, intermolecular interactions determine to a large extent the optoelectronic properties of thin solid films, the state in which organic semiconductors are applied in devices.⁶ Optimization of intermolecular charge and exciton transport is of critical importance for application of organic materials in field effect transistors, light-emitting diodes, and solar cells, since charge and exciton transport generally involves multiple molecules. Therefore, the organization in the material on a supramolecular scale plays an important role in organic semiconductors.

A natural strategy to control the ordering in a material on the molecular scale is to exploit molecular self-assembly.^{7–11} In this approach, molecular building blocks self-organize into complex, relatively well-defined structures through intermolecular interactions such as aromatic π -stacking, hydrogen bonding and electrostatic interactions.

An interesting example of such a material are the hydrogen-bonded dimers of phenylene vinylene oligomers (MOPVn) in Figure 1. In aliphatic hydrocarbon solvents these dimers self-assemble into chiral π -stacks that have been shown to be relatively efficient pathways for exciton transport.^{12,13} The transport efficiency of charges and excitons in such stacks critically depends on the electronic interactions between neighboring molecules. Although the aggregates formed are relatively

well-ordered, the degree of organization is still expected to be considerably less than in organic molecular crystals.

The charge transport properties of fibers of π -stacked MOPVs have been investigated recently by Durkut et al. who deposited MOPV stack fibers on a grid of electrodes with a spacing of 100 nm.¹⁴ However, to date, no current has been measured through these fibers.¹⁴ This raises the question whether the self-assembled helical structure that is formed in solution is retained when the fibers are transferred from solution to the substrate. Although the transfer of the stacks to a substrate has been demonstrated under certain circumstances,¹⁵ and polarized microscopy measurements indicate that the internal organization of the OPV stacks is preserved,¹⁶ it cannot be ruled out that the organization of the stacks on a substrate differs from the organization in solution. Moreover, in a device setup complications can occur since the charges have to overcome the injection barriers at the contacts. Therefore, it is of considerable interest to study the charge transport properties of the π -stacked MOPVs in solution using the electrodeless time-resolved microwave conductivity technique (TRMC). With the use of the TRMC technique, the conductivity due to charges on polymers or supramolecular aggregates in solution can be measured without the need to apply electrodes. This technique has been successfully used to measure the mobility of charges along several types of conjugated polymers.^{17–19}

In this work we used the time-resolved microwave conductivity technique to study the charge transport properties of MOPV4 stacks in solution. Additionally, we studied the charge transport properties using theoretical methods in order to gain more insight into the experimental results.

2. Experimental Methods

The experiments discussed here were performed on 1.8 mM solutions of the MOPV4 oligomer (see Figure 1) in *n*-hexane at room temperature. Under these conditions, MOPV4 dimers are present in the solution that self-assemble into stacks of MOPV4.¹⁵ Charge carriers were generated by irradiation of the MOPV4 solution with a 10 ns pulse of 3 MeV electrons from

* Corresponding author. E-mail: grozema@tnw.tudelft.nl.

[†] Delft University of Technology.

[‡] Eindhoven University of Technology.

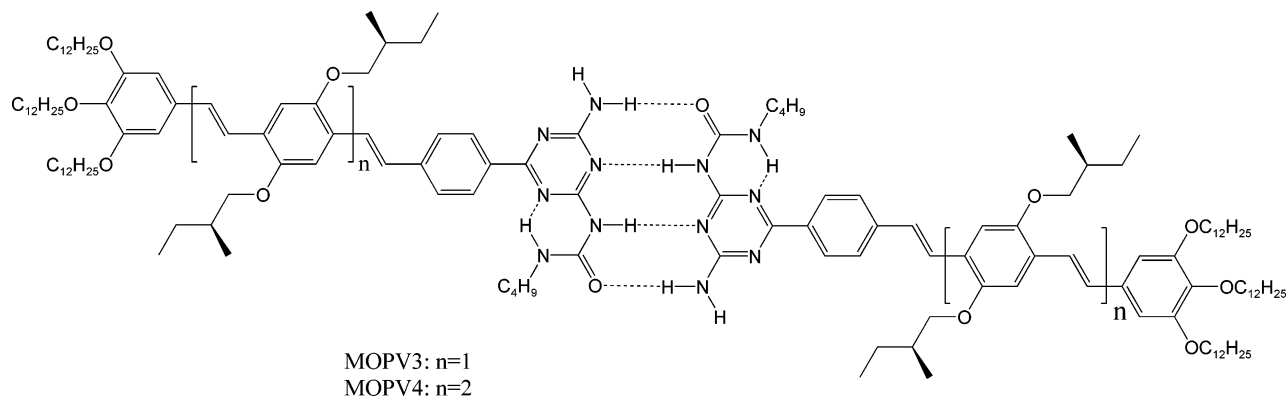


Figure 1. Molecular structure of hydrogen-bonded dimers of MOPV3 and MOPV4.

a Van de Graaff electron accelerator. The high-energy electrons scatter on the solvent molecules and produce a close to uniform distribution of excess electrons and *n*-hexane cations with a known concentration. These excess electrons and *n*-hexane cations can diffuse toward the MOPV4 stacks, where they undergo charge transfer because of the higher electron affinity and lower ionization potential of the stacks as compared to that of the solvent. This will lead to the formation of positively and negatively charged MOPV4 stacks, analogous to the experiments on derivatives of poly(phenylene vinylene).²⁰ The change in conductivity after the generation of charges was monitored on a nanosecond time scale by TRMC measurements at a frequency of 34 GHz.²¹ With this technique, the absorbance of microwave power as a result of the presence of (mobile) charges is monitored. In this way, we are able to determine the high-frequency mobility of charges on stacks of MOPV4 in solution, without the use of electrodes.^{17–20}

3. Computational Details

The rate for charge transfer between neighboring MOPVs, ν , can be evaluated using the Marcus equation:^{22–24}

$$\nu = \frac{J_{\text{eff}}^2(\theta, d)}{\hbar} \sqrt{\frac{\pi}{\lambda k_B T}} e^{-(\lambda/4k_B T)} \quad (1)$$

where λ is the reorganization energy and k_B is Boltzmann's constant. In this equation, J_{eff} is the effective charge-transfer integral, which is dependent on the stacking distance, d , and the mutual angle, θ , between adjacent MOPVs in the stack. This expression is equivalent to the hopping rate encountered in Holstein's theory for polaron hopping.²⁵ The parameters needed to calculate the charge-transfer rates using this equation (J_{eff} and λ) can be obtained from electronic structure calculations based on density functional theory (DFT). The semiclassical Marcus equation (eq 1) is a simplified form of the more general Levich–Marcus–Jortner equation which takes into account the effect of the quantum nature of vibrational modes on the charge-transfer rate through inclusion of the Huang–Rhys factor.²⁶ Use of the full equation does not alter the trends in the charge carrier mobility as a function of geometry changes but can lead to a modification of the mobility by a constant factor.

The geometries of the MOPV3 and MOPV4 oligomers containing a hydrogen-bonding unit (see Figure 1) were optimized by density functional theory calculations with the Amsterdam density functional (ADF) program.²⁷ The calculations were performed using the Becke–Perdew gradient-corrected exchange correlation functional and a triple- ζ plus

polarization (TZP) basis set consisting of Slater-type functions.²⁸ For calculations on open-shell systems (the cation and the anion) a restricted open-shell method was used.

The charge-transfer integrals at different angles between stacked MOPVs were calculated directly by density functional theory (DFT) using the fragment orbital approach in ADF. In this approach, the orbitals of a π -stacked dimer are expressed as a linear combination of the molecular orbitals of the individual OPV molecules. In this way, the charge-transfer integral, J , is directly obtained as the off-diagonal matrix element of the Kohn–Sham Hamiltonian matrix.²⁹ This method of calculating the charge-transfer integral gives direct and exact results and does not rely on the assumption of zero spatial overlap between the molecules as made when the charge-transfer integral is obtained from the orbital splitting. Moreover, in the method used here, it is not necessary to apply an electric field to bring the site energies of the molecules into resonance.^{30,31} The generalized or effective charge-transfer integral, to be used in calculations of charge transport, in which the spatial overlap is no longer explicitly taken into account, J_{eff} , is given by the following:³²

$$J_{\text{eff}} = J - \frac{1}{2}S(\epsilon_1 + \epsilon_2) \quad (2)$$

where S is the spatial overlap and ϵ_1 and ϵ_2 are the (absolute) energies for a charge localized on sites 1 and 2 (the site energy), respectively.

To calculate the reorganization energy, λ , for hole transfer the total energy of the cation and the neutral molecule were evaluated in both the neutral and the cation geometry. The reorganization energy, λ , is then given by the following:³³

$$\lambda = [E^+(g^0) - E^+(g^+)] + [E^0(g^+) - E^0(g^0)] \quad (3)$$

where $E^+(g^0)$ is the total energy of the cation in the neutral geometry, etc. The reorganization energy for the anion is calculated analogously. Note that we only consider the internal reorganization energy due to deformations of the MOPV molecules. The solvent reorganization energy is not taken into account, since the experiments to which we compare the calculated results were performed in *n*-hexane. In this solvent, the static and optical dielectric constant are virtually the same so that the solvent reorganization energy is negligible.³⁴

With the use of the charge-transfer integrals and the reorganization energies calculated by DFT, the rate for charge transfer between neighboring MOPVs can be calculated using eq 1. For a regular sequence of stacked molecules, all charge-transfer integrals, J_{eff} , along the stack are equal. In this case the charge

carrier mobility, μ , can be calculated directly by the following:

$$\mu = \frac{e}{k_B T} \nu d^2 \quad (4)$$

where d is the distance between neighboring localization sites, i.e., the stacking distance between adjacent MOPVs, and e is the elementary charge. The method to calculate the charge carrier mobility in molecular organic semiconductors as discussed above is similar to the methods used by other authors for the calculation of charge carrier mobility in π -stacked systems, e.g., the work by Brédas and co-workers.^{35,36}

For disordered stacks of MOPVs the charge-transfer integrals along the stack can differ from place to place, depending on the twist angles. In this case the mobility was calculated numerically by performing Monte Carlo simulations of polaron-hopping transport. The π -stack is represented by a sequence of localization sites that is sufficiently long so that the charge does not reach the chain ends on the time scale of the simulation. The charge is allowed to move from site to site by incoherent hopping with a hopping rate that is equal to the Marcus charge-transfer rate in eq 1. The angles were sampled uniformly from an interval around the equilibrium angle of 12° as estimated from quantum chemical calculations and fluorescence experiments.¹⁵ The time dependence of the twist angle was taken into account by assuming rotational diffusion of the hydrogen-bonded dimer on a flat potential energy surface centered on the equilibrium angle of 12° between infinitely high potential walls. The rotational motion is characterized by the rotational diffusion time, τ , the time in which the mean-squared angular deviation is 1 square radian, i.e.,

$$\langle \theta^2(t) \rangle = \frac{t}{\tau} \quad (5)$$

During the hopping simulation the mean-squared displacement $\langle x^2(t) \rangle$ of the charge along the π -stack was monitored as a function of time. In the case of normal diffusion of the charge in one dimension, the mean-squared displacement increases linearly in time:

$$\langle x^2(t) \rangle = 2Dt \quad (6)$$

where D is the diffusion constant of the charge on the π -stack. The charge carrier mobility is related to the diffusion constant by the Einstein relation:

$$\mu = \frac{eD}{k_B T} \quad (7)$$

4. Results

4.1. Time-Resolved Microwave Conductivity Measurements. In Figure 2 we present the conductivity upon irradiation for degassed *n*-hexane and for a degassed solution of *n*-hexane with stacks of the MOPV4 shown in Figure 1. The conductivity initially increases during the 10 ns electron pulse, as a result of the generation of charge carriers. Subsequently, the conductivity decreases due to recombination of positive and negative charges and by trapping of the charges on spurious impurities. The observed conductivity for degassed *n*-hexane is attributed to the excess electrons which have a mobility $\mu_e = 70 \times 10^{-3} \text{ cm}^2/(\text{V s})$.³⁷ The contribution of the *n*-hexane cations to the conductivity is negligible, since they have a much lower mobility of approximately $10^{-3} \text{ cm}^2/(\text{V s})$.³⁸ Recombination of the excess

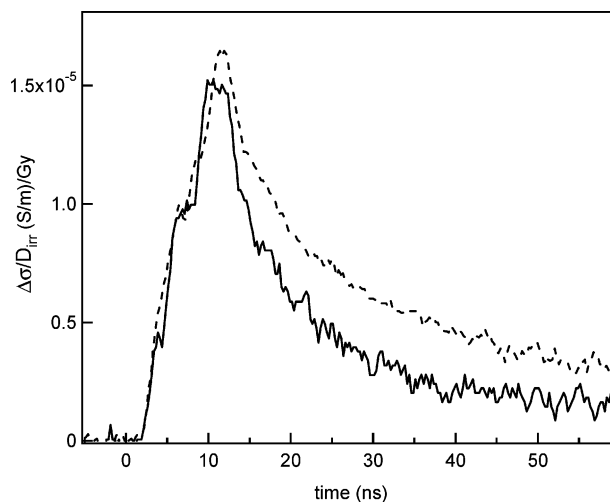


Figure 2. Change in conductivity, $\Delta\sigma$, upon irradiation of degassed *n*-hexane (dotted line) and a solution of degassed *n*-hexane with 1.8 mM MOPV4 oligomers (solid line) at an irradiation dose (D_{irr}) of 20 Gy.

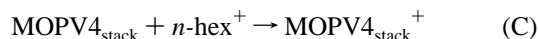
electrons, e^- , and *n*-hexane cations, $n\text{-hex}^+$, leads to a decay of the conductivity.



The decay of the conductivity in the degassed solution of *n*-hexane with stacks of MOPV4 is clearly faster than the decay for pure *n*-hexane, see Figure 2. The faster decay is attributed to transfer of excess electrons to MOPV4 stacks:



The *n*-hexane cations will also undergo charge transfer to the MOPV4 stacks:



Reaction C will occur since the ionization energy of MOPV4 molecules is lower than that of *n*-hexane. This reaction is analogous to the transfer of positive charge observed earlier for oligo(phenylene vinylene) derivatives in benzene solution.³⁹ The difference between the conductivity transient for pure *n*-hexane and the MOPV4 solution in *n*-hexane (Figure 2) is a result of the transfer of charges to the MOPV4 molecules in the solution by reactions B and C. This charge transfer occurs in competition with the homogeneous recombination of positive and negative charges by reaction A. The fact that the conductivity in a solution of MOPV4 in *n*-hexane (due to the mobility of electrons in *n*-hexane) decays faster than in pure *n*-hexane means that the negative charges (and holes) transfer to a species where they have a lower mobility than electrons in *n*-hexane. This provides a direct indication that the (sum of the) mobilities for electrons and holes on MOPV4 stacks is smaller than the mobility of excess electrons in *n*-hexane ($70 \times 10^{-3} \text{ cm}^2/(\text{V s})$).

Additional experiments were performed on oxygen-saturated *n*-hexane solutions of MOPV4. Due to the relatively high concentration (18 mM) and electron affinity of oxygen, the excess electrons generated during the electron pulse rapidly react with the oxygen molecules to form oxygen anions with a low mobility:⁴⁰



The conductivity of oxygen-saturated *n*-hexane solutions containing MOPV4 stacks was found to be comparable to the conductivity for oxygen-saturated *n*-hexane. In the first case positive charges will be present on the MOPV4 stacks as argued above, while in the latter case only *n*-hexane cations are present. The similarity of the conductivity in both solutions indicates that the mobility of holes on MOPV4 stacks has to be comparable to the mobility of *n*-hexane cations; i.e., $\approx 10^{-3} \text{ cm}^2/(\text{V s})$.³⁸

The mobility values given so far are isotropic mobilities, μ_{iso} . Since charges moving along the MOPV4 stacks are only mobile along the direction of the stack, the mobility of interest is the one-dimensional mobility $\mu_{1\text{D}}$. Taking into account the random orientation of the stacks in solution and the linear polarization of the microwave field, the one-dimensional mobility is given by $\mu_{1\text{D}} = 3\mu_{\text{iso}}$.¹⁹

A kinetic analysis of the conductivity transients for the *n*-hexane solution containing MOPV4 stacks in Figure 2, involving the reactions A–C were performed in the same way as previously described.²⁰ The most important parameters involved in this kinetic analysis are the reaction rates for reactions B and C and the mobility of charges on the stacks. The conductivity measured for the MOPV4 solutions was rather small compared to those generally obtained for conjugated polymers.^{17–19} However, we can still give an estimate of mobility of positive and negative charges on MOPV4 stacks. The values found for the hole and electron mobility along the MOPV4 stack are $3 \times 10^{-3} \text{ cm}^2/(\text{V s})$ and $9 \times 10^{-3} \text{ cm}^2/(\text{V s})$, respectively.

The reaction rates of reactions B and C are of interest since they contain information about the size of the molecular species to which the charges are transferred. This is especially interesting since the formation and breaking up of the MOPV4 stacks is a dynamic process. For a given temperature and MOPV4 concentration, an equilibrium will be established between MOPV4 dimers in solution and MOPV4 dimers in a stack.¹⁵ Using the charge-transfer reaction kinetics, we can determine whether the charges are transferred to MOPV4 stacks or to individual MOPV4 dimers. From the kinetic analysis we have obtained the reaction rate for the transfer of (negative) charge to the MOPV4 stacks. This rate, k , is given by $k = 4\pi R_{\text{eff}} D_{\text{e}}$, where R_{eff} is the effective reaction radius of the MOPV4 stack and $D_{\text{e}} = \mu_{\text{e}} k_{\text{B}} T / e$ is the diffusion constant of the excess electron in *n*-hexane. From the rate constant obtained from the kinetic analysis of the conductivity transients in Figure 2, we find an effective reaction radius of the MOPV4 stack of about 10 nm. The effective reaction radius determined from the kinetic analysis can be compared to the effective reaction radius expected on the basis of the stack dimensions. From the length of a stack as found with SANS experiments (150 nm)¹⁵ and the stacking distance between adjacent MOPV4 dimers (3.5 Å), we find that a stack consist of about 450 MOPV4 dimers. The effective reaction radius for an object that can be represented by a linear array of reacting units was discussed by Traytak.^{41–43} The effective reaction radius, R_{eff} , for large n can be approximated by $R_{\text{eff}} = na/(2 \ln(n))$, where a is the distance between the centers of the reacting units.²⁰ Taking 3.5 Å as the distance between the units (the stacking distance) and the number of dimers in a stack determined from experiments (450) for n , a value of 12 nm is obtained for the effective reaction radius of an MOPV4 stack. The calculated value for the effective reaction radius of the MOPV4 stack is in good agreement with the value of 10 nm found from the kinetic analysis, thus

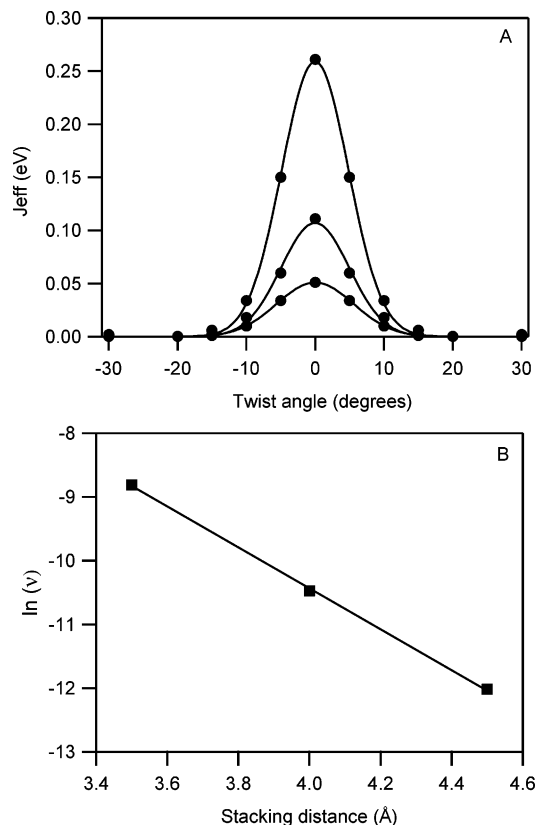


Figure 3. (A) Dependence of the effective charge-transfer integral, J_{eff} , on the twist angle for MOPV3 at stacking distances of 3.5, 4, and 4.5 Å (from top to bottom). (B) Natural logarithm of the charge-transfer rate, v , plotted against the stacking distance with a twist angle of zero degrees.

confirming the presence of MOPV4 stacks in the *n*-hexane solution and the transfer of electrons to these stacks.

4.2. Charge Transport Calculations. The charge-transfer integral or electronic coupling between stacked MOPVs was calculated for a variety of twist angles and stacking distances. The twist angle is defined as the mutual angle between two stacked dimers, where the center of mass (between the two hydrogen-bonding units) is the center of rotation. In this work we are interested in the motion of electrons and holes along the stacks. Therefore, the effective charge-transfer integrals were calculated for the highest occupied molecular orbital (HOMO) and the lowest unoccupied molecular orbital (LUMO), the relevant orbitals for hole and electron transport, respectively. In Figure 3 the effective charge-transfer integral, J_{eff} , for the HOMOs is plotted for MOPV3 as a function of the twist angle for different stacking distances. The coupling is maximal for a zero twist angle, where the overlap is optimal. For all stacking distances J_{eff} rapidly decays with increasing twist angle and becomes close to zero for angles larger than 15° . Note that the effective charge-transfer integrals were calculated between two stacked MOPV molecules in the same "strand" and not between two dimers of MOPVs. Since the electronic couplings through the hydrogen bonds are very small (0.0002 and 0.004 eV for the hole and electron, respectively) the HOMO and LUMO orbitals will be localized on a single molecule rather than delocalized over both molecules in a dimer. The effective charge-transfer integral between two diagonal MOPV molecules, i.e., MOPV molecules located in different strands and in different dimers, are even smaller ($3 \times 10^{-5} \text{ eV}$ for both the electron and the hole). Therefore, this pathway for charge transport was not included in the calculations presented here.

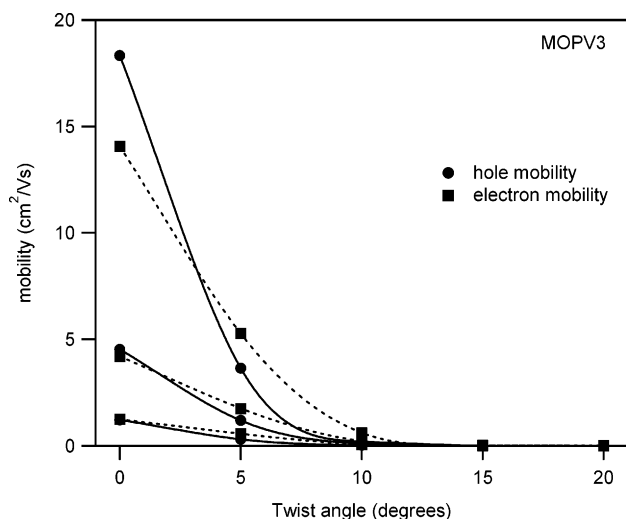


Figure 4. Dependence of the electron and hole mobility on the twist angle in stacks of MOPV3 at stacking distances of 3.5, 4, and 4.5 Å (from top to bottom).

The reorganization energies were calculated by DFT as discussed in section 3. For MOPV3 the reorganization energies were found to be 0.20 and 0.25 eV for the hole and the electron, respectively. For MOPV4 both reorganization energies were smaller; 0.16 and 0.20 eV, for the hole and the electron, respectively. The smaller reorganization energy for the electron and the hole on MOPV4 reflect the more delocalized nature of the charge on the longer oligomer. The net charge per phenylene vinylene (PV) unit is smaller for MOPV4 (see also Figure 7 for the charge distributions obtained from DFT calculations), and therefore the geometry deformations induced by the charge are less.

The effective charge-transfer integrals and reorganization energies were used to calculate the charge-transfer rate according to eq 1. The charge-transfer rate decreases exponentially with the stacking distance as can be seen in Figure 3B for a zero twist angle. If the exponential distance dependence of the charge-transfer rate, ν , is considered ($\nu \sim e^{-\beta R}$) a decay constant β of 3.2 \AA^{-1} is obtained. This is a typical value for charge transfer through vacuum.^{44,45}

The charge carrier mobility for electrons and holes along stacks of MOPV3 and MOPV4 as a function of the twist angle and the stacking distance were calculated using the charge-transfer rate in eq 1 and the expression for the mobility in eq 4. The results are shown in Figures 4 and 5 for MOPV3 and MOPV4, respectively. For MOPV3 the calculated mobility of holes along the stack is close to $18 \text{ cm}^2/(\text{V s})$ for a twist angle of zero degrees and a stacking distance of 3.5 Å. Experimental results show that the MOPVs self-assemble into a helical geometry with nonzero twist angle.¹⁵ Increasing the twist angle from zero degrees leads to a dramatic decrease of the charge carrier mobility; the hole mobility at 10° was calculated to be $0.20 \text{ cm}^2/(\text{V s})$ for MOPV3, i.e., 100 times smaller than the mobility at zero degrees. Increasing the twist angle further to 15° leads to an additional lowering of the mobility by a factor of 50 to $0.004 \text{ cm}^2/(\text{V s})$. The electron mobility also exhibits a strong decrease with increasing twist angle; however, the decrease is less pronounced than that for the holes. The electron mobility decreases by approximately a factor of 20 when going from zero to 10° , compared to a factor of 100 for the hole mobility. The charge carrier mobilities also depend quite strongly on the stacking distance as expected from the strong decrease of the effective charge-transfer integral with increasing distance (Figure 3).

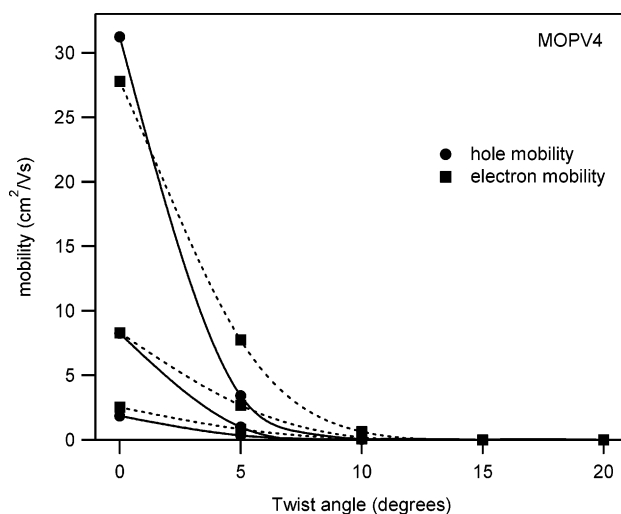


Figure 5. Dependence of the electron and hole mobility on the twist angle in stacks of MOPV4 at stacking distances of 3.5, 4, and 4.5 Å (from top to bottom).

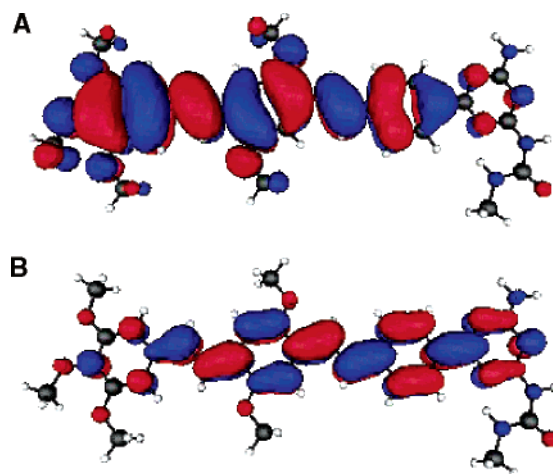


Figure 6. HOMO (A) and LUMO (B) orbitals of MOPV3.

Similar results are obtained for calculations on MOPV4. In this case the mobility was calculated to be close to $30 \text{ cm}^2/(\text{V s})$ for zero twist angle and a stacking distance of 3.5 Å. The decrease in mobility when going to an angle of 10° is even larger than for MOPV3; the mobility was reduced by a factor of ~ 700 in this case. Also for MOPV4 the electron mobility decays slower with increasing twist angle than the hole mobility.

The different dependence of the mobility on the twist angle for the electron as compared to that for the hole can be understood when we examine the molecular orbitals relevant for hole and electron transport. In Figure 6 the HOMO and LUMO orbitals are shown for MOPV3. The HOMO is located on the PV part of the molecules with highest density toward the end phenyl unit, which is substituted with three alkoxy chains. The contribution of atomic orbitals on the hydrogen-bonding unit to the HOMO orbital is negligible. For the LUMO the situation is reversed; there is hardly any density on the end phenyl unit while there is a substantial contribution of orbitals on the hydrogen-bonding unit. These results are consistent with previous calculations on alkoxy-substituted oligo-PVs where it was found that positive charges tend to localize on phenyl rings containing alkoxy side chains rather than on unsubstituted phenyl groups.³⁹ The shape of the HOMO and LUMO orbitals provides a representative picture of the charge distributions of the positive and negative charge on the MOPV chains. This can be seen in Figure 7 where the changes in the positive and

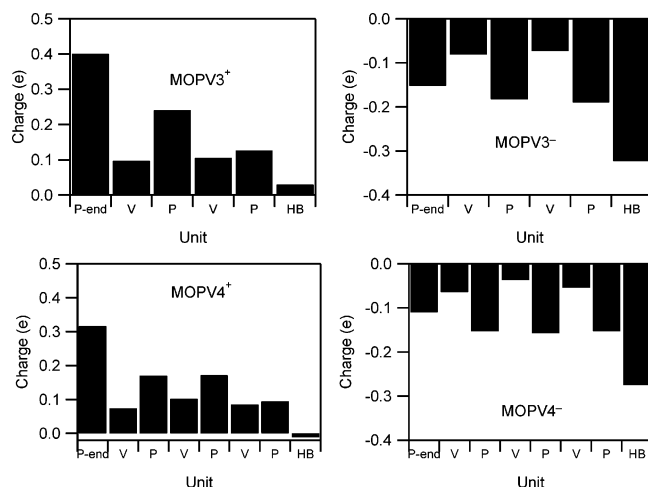


Figure 7. Charge distribution on positively and negatively charged MOPV3 and MOPV4. The phenylene and vinylene units and the hydrogen-bonding unit are indicated by P, V, and HB, respectively.

negative charge on the phenylene and vinylene units in MOPV3 and MOPV4 cations and anions are shown. The charges were obtained by adding the Mulliken charges obtained from DFT calculations on all atoms in a phenylene or vinylene unit and subtracting the charge that was present on that unit in the neutral molecule. For both MOPV3 and MOPV4 the positive charge is localized mostly at the end phenyl group that contains three alkoxy side chains, whereas the negative charge is mostly localized at the hydrogen-bonding unit. The spatial distribution of the charges and of the HOMO and LUMO orbitals gives a direct indication of the difference in the angular dependence of the hole and electron mobility. The hole is localized at the chain ends, far away from the center of rotation which causes the overlap between the HOMO orbitals to decrease rapidly with increasing angle. The electron is localized close to the center of rotation at the hydrogen-bonding unit. Therefore the overlap decreases slower with increasing angles. By the same token, the hole mobility in MOPV4 decays faster with increasing angle than the hole mobility in MOPV3 since the localization site of the hole is further from the rotation center for MOPV4.

In the mobility calculations discussed so far, it was assumed that the stack of MOPV molecules forms a helical structure with a fixed twist angle between neighboring hydrogen-bonded dimers. In reality, however, the stacks are likely to exhibit significant deviations from such a perfectly regular structure. The deviations can be both of static and of dynamic nature. To examine the effect of structural fluctuations on the charge carrier mobility, we have performed polaron-hopping calculations in which structural fluctuations are accounted for. In the simulations dynamic fluctuations of the twist angles between neighboring MOPV dimers are taken into account. This type of fluctuation is expected to have the largest effect on the charge carrier mobility, larger than fluctuations in the stacking distance. Fluctuations in the twist angles lead to variations of the hopping rates between neighboring MOPV4 molecules along the stack. The angles between neighboring molecules were evenly distributed between 7° and 17° , a symmetrical interval of angles around the equilibrium angle of 12° that was derived from previous studies.¹⁵ In our model, the twisting dynamics of the MOPV dimers in the stacks is described by rotational diffusion which is characterized by a rotational diffusion time, see section 3. The rotational diffusion time for an elongated molecule can be estimated by considering the rotational friction coefficients of a cylinder in a solvent with a certain viscosity.⁴⁶ If the shape of the molecule is assumed to be a cylinder with a long axis of

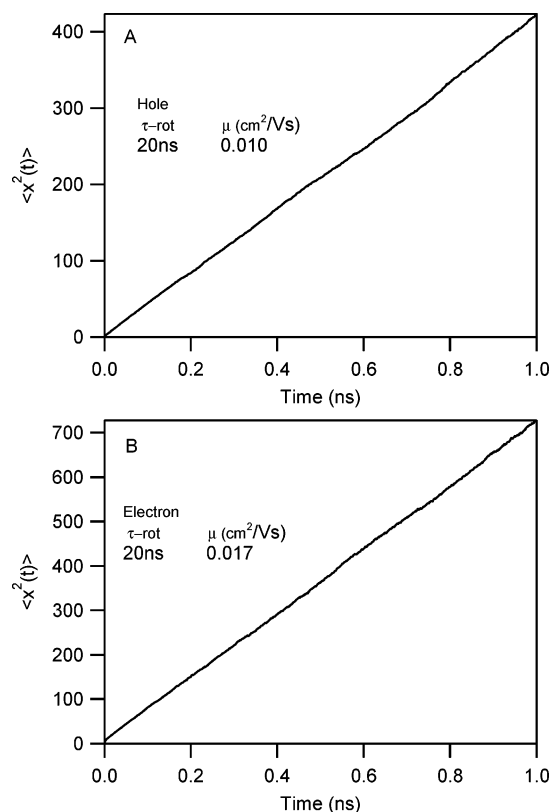


Figure 8. Calculated mean-squared displacement of a hole (A) and an electron (B) along a dynamic MOPV4 stack with a stacking distance of 3.5 \AA as a function of time for a rotational diffusion time of 20 ns.

60 \AA , the length of an MOPV4 dimer without side chains, and a width of 5.5 \AA , a "tumbling" rotation time of 5 ns is obtained. If the length of the cylinder is taken to be twice as large (120 \AA) in order to take the long side chains into account, a rotation time of 30 ns is obtained. It should be noted that these rotation times are approximate values and serve only as an indication of the order of magnitude for the real rotation time. During the hopping simulations the mean-squared displacement $\langle x^2(t) \rangle$ of the charge was monitored as a function of time. Examples of the time dependence of the mean-squared displacement are shown in Figure 8. The mean-squared displacement is shown for a rotational diffusion time of 20 ns. For all cases considered the mean-squared displacement was found to increase linearly with time after the initial stages of the transport. Therefore, the diffusion constant, D , of the charge carrier can be obtained from the slope of the curves in Figure 8, as discussed in section 3. The charge carrier mobility is directly proportional to the diffusion constant by the Einstein relation (eq 7). The mobility for a positive charge, obtained from the simulations with a rotational diffusion time of 20 ns, is $0.010 \text{ cm}^2/(\text{V s})$. For this relatively long rotation time the mobility appears to be limited by the largest angles in the interval. The calculated hole mobility of around $0.01 \text{ cm}^2/(\text{V s})$ found for twist angles fluctuating between 7° and 17° is the same as the mobility for a static stack with interunit angles of 17° at the same stacking distance.

The calculated mobility for the electron is somewhat higher than for the hole; $0.017 \text{ cm}^2/(\text{V s})$ for a rotation time of 20 ns. This value is again close to the value calculated for the static π -stack with a fixed twist angle of 17° . Also in this case, the larger angles dominate the charge transport since the mobility for the case of fixed twist angles close to 12° has a much higher value close to $0.5 \text{ cm}^2/(\text{V s})$.

The results discussed above show, that on the time scale of charge transport, the disorder in the stacks is almost of a static

nature for the rotation times used here. Charge transport within regions with relatively small twist angles is very fast, and the charge is only hindered by sites with small charge-transfer integrals. The twisting motion with a rotation time of 20 ns already appears to be too slow to twist the stacked MOPVs back to a smaller angle on the time scale on which the charge transport takes place.

5. Discussion

The calculated charge carrier mobilities of electrons and holes along regular static π -stacks of hydrogen-bonded MOPV dimers with a twist angle of 12° ($0.65 \text{ cm}^2/(\text{V s})$ for the electron and $0.04 \text{ cm}^2/(\text{V s})$ for the hole) are up to a few orders of magnitude higher than the values deduced experimentally with TRMC measurements ($9 \times 10^{-3} \text{ cm}^2/(\text{V s})$ for the electron and $3 \times 10^{-3} \text{ cm}^2/(\text{V s})$ for the hole). If the mobilities were indeed as high as the calculated values the microwave conductivity due to electrons and positive charges on the MOPV stacks should have been significantly higher than the measured results. This means that there is likely to be a considerable amount of conformational disorder along the stacks, which has a limiting effect on charge transport. The polaron-hopping calculations show that we obtain mobilities that are comparable to the experimentally deduced values if it is assumed that there is a distribution of twist angles around the average twist angle of 12° .¹⁴ It should be noted that a direct quantitative comparison of the experimental and calculated mobility should be done with care because of the (unavoidable) approximations made in the calculated mobilities. One of the approximations made is the neglect of the quantum nature of vibrations on the charge-transfer rate by using an approximate form of the Levich–Marcus–Jortner equation as mentioned in section 3. We can estimate the change in the charge-transfer rate due to the quantum nature of the vibrational modes by taking the Huang–Rhys factor equal to 1 (a typical value for conjugated materials⁴⁷) and a typical value for the vibration energy for a C–C stretch vibration (0.2 eV). This leads to a lowering of the charge-transfer rate by at most a factor three. As noted section 3, this does not alter the trend of the mobility as a function of the twist angle.

From the calculations presented here it is clear that conformational disorder can decrease the charge carrier mobility by more than an order of magnitude. In the calculations discussed above we have considered two types of conformational fluctuations, the twist angle between neighboring MOPV dimers and the stacking distance.

The calculations presented above show that deviations in the twist angle of only a few degrees already have a large effect on the charge carrier mobility. Fluctuations in the twist angles between 7° and 17° decrease the mobility by an order of magnitude or more, as compared to the results for a static stack with twist angles of 12° . Although the circular dichroism (CD) spectra of the MOPV stacks suggest the presence of a left-handed helical arrangement of MOPV molecules,¹⁴ it cannot be ruled out that there are considerable deviations from a regular helical structure. With conformational fluctuations of up to 5° , the π -stacks can still retain their chiral helical conformation that gives rise to the features observed in the CD spectrum.

It was shown that increasing the stacking distance leads to a smaller charge carrier mobility; however, it is not expected that the stacking distance will increase beyond 4 Å. Therefore, we expect the effect of the stacking distance to be smaller than that of fluctuations in the twist angles.

Apart from the fluctuation in the twist angle and the stacking distance, there may also be other conformational fluctuations,

such as, e.g., shifting of the dimers with respect to each other or even geometrical distortions of the hydrogen-bonded dimers themselves. All of these fluctuations are expected to reduce the charge carrier mobility.

The calculations that we performed also show that the charge carrier mobility in self-organizing π -stacks can be increased by several orders of magnitude if a supramolecular organization can be achieved that is more favorable for charge transport. In the case of the hydrogen-bonded MOPV4 dimer stacks considered here, this means that the twist angle should be decreased so that it becomes closer to the angle that is optimal for charge transport, i.e., a zero degree angle. The twist angle between the π -stacked dimers can possibly be decreased by modifications in the side chains so that the steric repulsion between the side chains is reduced. Alternatively, the introduction of additional functional groups that, for instance, enable hydrogen bonding in the π -stacking direction, can also provide a route to supramolecular aggregates with a more ordered structure. Hydrogen bonding between π -stacked molecules has been explored previously in discotic materials and in stacks of oligothiophenes and was shown to result in significant improvement of the charge transport properties of such materials.^{48,49}

6. Conclusions

The mobility of positive and negative charges along self-organizing π -stacks of hydrogen-bonded dimers of phenylene vinylene oligomers was studied experimentally by microwave conductivity measurements. The charge carrier mobilities deduced from the experimental data are $9 \times 10^{-3} \text{ cm}^2/(\text{V s})$ and $3 \times 10^{-3} \text{ cm}^2/(\text{V s})$ for the electron and the hole, respectively.

We have also calculated the charge carrier mobility using a hopping model with parameters obtained from density functional theory calculations. The mobility was calculated for regular static π -stacks with varying twist angles and stacking distances between neighboring oligomers. It was found that the mobility strongly depends on the twist angle between neighboring dimers in the stack. To reproduce the experimentally measured mobility it had to be assumed that there is considerable disorder in the twist angles along the stack. With a distribution of twist angles between 7° and 17° the experimentally deduced values for the charge carrier mobility could be reproduced. Based on the calculations, we conclude that an increase in the charge carrier mobility of a few orders of magnitude could be achieved in these self-organizing aggregates if the amount of disorder can be reduced so that the occurrence of larger twist angles is avoided.

Acknowledgment. This work was supported by The Netherlands Foundations for Fundamental Research on Matter (FOM) and The Netherlands Organization for Scientific Research (NWO).

References and Notes

- (1) Sirringhaus, H.; Brown, P. J.; Friend, R. H.; Nielsen, M. M.; Bechgaard, K.; Langeveld-Voss, B. M. W.; Spiering, A. J. H.; Janssen, R. A. J.; Meijer, E. W.; Herwig, P.; de Leeuw, D. M. *Nature* **1999**, *401*, 685.
- (2) Burroughes, J. H.; Bradley, D. D. C.; Brown, A. R.; Marks, R. N.; MacKay, K.; Friend, R. H.; Burns, P. L.; Holmes, A. B. *Nature* **1990**, *347*, 539.
- (3) Winder, C.; Sariciftci, N. S. *J. Mater. Chem.* **2004**, *14*, 1077.
- (4) Padmanaban, G.; Ramakrishnan, S. *J. Am. Chem. Soc.* **2000**, *122*, 2244.
- (5) van Hutten, P. F.; Krasnikov, V. V.; Hadzioannou, G. *Acc. Chem. Res.* **1999**, *32*, 257.
- (6) Kim, J. *Pure Appl. Chem.* **2002**, *74*, 2031.
- (7) Lehn, J.-M. *Rep. Prog. Phys.* **2004**, *67*, 249.

- (8) Lehn, J.-M. *Polym. Int.* **2002**, *51*, 825.
- (9) Elemans, J. A. A. W.; Rowan, A. E.; Nolte, R. J. M. *J. Mater. Chem.* **2003**, *13*, 2661.
- (10) Leclère, P.; Surin, M.; Jonkheijm, P.; Henze, O.; Schenning, A. P. H. J.; Biscarini, F.; Grimsdale, A. C.; Feast, W. J.; Meijer, E. W.; Müllen, K.; Brédas, J.-L.; Lazzaroni, R. *Eur. Polym. J.* **2004**, *40*, 885.
- (11) Schenning, A. P. H. J.; Jonkheijm, P.; Hoeben, F. J. M.; Herrikhuysen, J. V.; Meskers, S. C. J.; Meijer, E. W.; Herz, L. M.; Daniel, C.; Silva, C.; Phillips, R. T.; Friend, R. H.; Beljonne, D.; Miura, A.; De Feyter, S.; Zdanowska, M.; Uji-i, H.; De Schryver, F. C.; Chen, Z.; Würthner, F.; Mas-Torrent, M.; den Boer, D.; Durkut, M.; Hadley, P. *Synth. Met.* **2004**, *147*, 43.
- (12) Herz, L. M.; Daniel, C.; Silva, C.; Hoeben, F. J. M.; Schenning, A. P. H. J.; Meijer, E. W.; Friend, R. H.; Phillips, R. T. *Phys. Rev. B* **2003**, *68*, 045203.
- (13) Beljonne, D.; Hennebicq, E.; Daniel, C.; Herz, L. M.; Silva, C.; Scholes, G. D.; Hoeben, F. J. M.; Jonkheijm, P.; Schenning, A. P. H. J.; Meskers, S. C. J.; Phillips, R. T.; Friend, R. H.; Meijer, E. W. *J. Phys. Chem. B* **2005**, *109*, 10594.
- (14) Durkut, M.; Mas-Torrent, M.; Hadley, P.; Jonkheijm, P.; Schenning, A. P. H. J.; Meijer, E. W.; George, S.; Ajayaghosh, A. Submitted for publication, 2005.
- (15) Jonkheijm, P.; Hoeben, F. J. M.; Kleppinger, R.; Van Herrikhuysen, J.; Schenning, A. P. H. J.; Meijer, E. W. *J. Am. Chem. Soc.* **2003**, *125*, 15941.
- (16) Jeukens, C. R. L. P.; Jonkheijm, P.; Wijnen, F. J. P.; Gielen, J. C.; Christiansen, P. C. M.; Schenning, A. P. H. J.; Meijer, E. W.; Maan, J. C. *J. Am. Chem. Soc.*, in press.
- (17) Hoofman, R. J. O. M.; de Haas, M. P.; Siebbeles, L. D. A.; Warman, J. M. *Nature* **1998**, *392*, 54.
- (18) Grozema, F. C.; Siebbeles, L. D. A.; Warman, J. M.; Seki, S.; Tagawa, S.; Scherf, U. *Adv. Mater.* **2002**, *14*, 228.
- (19) Prins, P.; Candeias, L. P.; Van Breemen, A. J. J. M.; Sweelssen, J.; Herwig, P. T.; Schoo, H. F. M.; Siebbeles, L. D. A. *Adv. Mater.* **2005**, *17*, 718.
- (20) Grozema, F. C.; Hoofman, R. J. O. M.; Candeias, L. P.; de Haas, M. P.; Warman, J. M.; Siebbeles, L. D. A. *J. Phys. Chem. A* **2003**, *107*, 5976.
- (21) Infelta, P. P.; de Haas, M. P.; Warman, J. M. *Radiat. Phys. Chem.* **1977**, *10*, 353.
- (22) Bixon, M.; Jortner, J. *Chem. Phys.* **2002**, *281*, 393.
- (23) Mikkelsen, K. V.; Ratner, M. A. *Chem. Rev.* **1987**, *87*, 113.
- (24) Marcus, R. A.; Sutin, N. *Biochim. Biophys. Acta Rev. Bioenerg.* **1985**, *811*, 265.
- (25) Holstein, T. *Ann. Phys.* **1959**, *8*, 343.
- (26) Bixon, M.; Jortner, J. *Adv. Chem. Phys.* **1999**, *106*, 35.
- (27) te Velde, G.; Bickelhaupt, F. M.; Baerends, E. J.; Fonseca Guerra, C.; van Gisbergen, S. J. A.; Snijders, J. G.; Ziegler, T. *J. Comput. Chem.* **2001**, *22*, 931.
- (28) Snijders, J. G.; Vernooijs, P.; Baerends, E. J. *At. Data Nucl. Data Tables* **1981**, *26*, 483.
- (29) Senthilkumar, K.; Grozema, F. C.; Bickelhaupt, F. M.; Siebbeles, L. D. A. *J. Chem. Phys.* **2003**, *119*, 9809.
- (30) Voityuk, A. A.; Rösch, N. *J. Chem. Phys.* **2002**, *117*, 5607.
- (31) Voityuk, A. A.; Jortner, J.; Bixon, M.; Rösch, N. *J. Chem. Phys.* **2001**, *114*, 5614.
- (32) Newton, M. D. *Chem. Rev.* **1991**, *91*, 767.
- (33) Tavernier, H. L.; Fayer, M. D. *J. Phys. Chem. B* **2000**, *104*, 11541.
- (34) Kavarnos, G. J. *Fundamentals of Photoinduced Electron Transfer*; VCH Publishers: New York, 1993.
- (35) Cornil, J.; Lemaire, V.; Calbert, J. P.; Brédas, J.-L. *Adv. Mater.* **2002**, *14*, 726.
- (36) Lemaire, V.; da Silva Filho, D. A.; Coropceanu, V.; Lehmann, M.; Geerts, Y.; Piris, J.; Debije, M. G.; van de Craats, A. M.; Senthilkumar, K.; Siebbeles, L. D. A.; Warman, J. M.; Brédas, J.-L.; Cornil, J. *J. Am. Chem. Soc.* **2004**, *126*, 3271.
- (37) Allen, A. O.; Holroyd, R. A. *J. Phys. Chem.* **1974**, *78*, 796.
- (38) Warman, J. M. The dynamics of electrons and ions in nonpolar liquids. In *The Study of Fast Processes and Transient Species by Electron Pulse Radiolysis*; Baxendale, J. H., Busi, F., Eds.; Reidel: Dordrecht, The Netherlands, 1982; p 433.
- (39) Grozema, F. C.; Candeias, L. P.; Swart, M.; van Duijnen, P. T.; Wildeman, J.; Hadziioannou, G.; Siebbeles, L. D. A.; Warman, J. M. *J. Chem. Phys.* **2002**, *117*, 11366.
- (40) Allen, A. O.; de Haas, M. P.; Hummel, A. *J. Chem. Phys.* **1976**, *64*, 2587.
- (41) Traytak, S. D. *Chem. Phys.* **1995**, *193*, 351.
- (42) Traytak, S. D. *Chem. Phys. Lett.* **1992**, *197*, 247.
- (43) Traytak, S. D. *Chem. Phys. Lett.* **1994**, *227*, 180.
- (44) Pullen, S. H.; Edington, M. D.; Studer-Martinez, S. L.; Simon, J. D.; Staab, H. A. *J. Phys. Chem. A* **1999**, *103*, 2740.
- (45) Miller, N. E.; Wander, M. C.; Cave, R. J. *J. Phys. Chem. A* **1999**, *103*, 1084.
- (46) Tirado, M. M.; Garcia de la Torre, J. *J. Chem. Phys.* **1980**, *73*, 1986.
- (47) Hagler, T. W.; Pakbaz, K.; Voss, K. F.; Heeger, A. J. *Phys. Rev. B* **1991**, *44*, 8652.
- (48) Schoonbeek, F. S.; Van Esch, J. H.; Wegewijs, B. R.; Rep, D. B. A.; de Haas, M. P.; Klapwijk, T. M.; Kellog, R. M.; Feringa, B. L. *Angew. Chem., Int. Ed.* **1999**, *38*, 1393.
- (49) Gearba, R. I.; Lehmann, M.; Levin, J.; Ivanov, D. A.; Koch, M. H. J.; Barbera, J.; Debije, M. G.; Piris, J.; Geerts, Y. H. *Adv. Mater.* **2003**, *15*, 1614.